Intelligent low-level RF system by non-destructive beam monitoring device for cyclotrons

M. S. Sharifi Asadi Malafeh[1] M. Ghergherehchi[1,2;1)]
H. Afarideh[1;2)] J. S. Chai[2] Yoon Sang Kim[3]

[1] Department of Energy Engineering & Physics, Amirkabir University of Technology, Tehran, Iran
[2] College of Information & Communication Engineering, Sungkyunkwan University, Suwon, Korea
[3] Schoot of Computer Science and Engineering, Korea University of Technology and Education, Cheonan, Korea

Abstract: The project of a 10 MeV PET cyclotron accelerator for medical diagnosis and treatment was started at Amirkabir University of Technology in 2012. The low-level RF system of the cyclotron accelerator is designed to stabilize acceleration voltage and control the resonance frequency of the cavity. In this work an Intelligent Low Level Radio Frequency Circuit or ILLRF, suitable for most AVF cyclotron accelerators, is designed using a beam monitoring device and narrow band tunable band-pass filter. In this design, the RF phase detection does not need signal processing by a microcontroller.

Keywords: ILLRF, beam monitoring device, reflected power, phase detector and resonance frequency variation

PACS: 29.20.dg, 29.25.Ni **DOI:** 10.1088/1674-1137/40/4/047001

1 Introduction

An Intelligent Low Level Radio Frequency (ILLRF) circuit is used in cyclotron accelerators to generate a signal, adjust the phase and frequency, and stabilize and protect the RF set from the reflected power due to changes in the resonance frequency of the cavity due to thermal cavity deformation [1]. Therefore, a noiseless RF signal must be generated, amplified and applied to the cavity in order to establish a suitable electric field. Noise and signal harmonics are inseparable parts of all high-frequency electronic circuits, so an appropriate filter must be used to eliminate harmonics and noise [2]. A narrow band tunable band-pass filter should be used because of the sensitivity of the system to the harmonics of the signal as well as noise. In a cyclotron, the variation in the resonant frequency of the cavity causes power to be reflected, so a reflected power detector (directional coupler) is used to tune the resonant frequency of the cavity and avoid such risk.

The cavity consists of two D-shaped regions known as Dees, a linear part, a stem and so on. When the variation of the resonant frequency of the cavity is negligible, the best way to detect the variation in the resonant frequency is to measure the phase difference of the forward signal and the sampled signal of the Dees using an RF phase detector. For this method, we only use a simple microcontroller for RF phase detection instead of using a microprocessor for signal processing. The lack of coherence between the beam rotational phase and RF signal phase will result in a loss of beam resolution. Therefore, we propose using a beam-monitoring device that determines the phase, position and current information of the beam to solve this problem.

A narrow band-pass filter is used to reduce the effect of noise and harmonics that cause a reduction in the overall bandwidth of the system. Therefore, an LLRF with a fixed narrow band-pass filter is generally designed for use in only one specific accelerator. However, our design uses a tunable band-pass filter with an ultra-narrow band pass, so the general bandwidth of the system does not decrease. The ILLRF circuit demonstrates a high level of intelligence by using the appropriate sub-blocks to predict all probable conditions. The ILLRF circuit is the start-up block of the RF section and consists of a Signal Generation and Adjustment Block with the help of Amplitude, Frequency and Phase Feedback Loops and a Beam-monitoring device to protect the system and adjust the RF signal. The ILLRF circuit consists of the following main blocks:

1) Signal generation and adjustment block

2) Amplitude, reflected power and phase feedback loops

3) Protection block

Received 14 September 2015

1) E-mail: mitragh@skku.edu

2) E-mail: hafarideh@aut.ac.ir

4) Automatic gain control block to stabilize the amplitude

5) Beam-monitoring device for beam phase, current, and position detection

The ILLRF with feedback, output and beam-monitoring devices is shown in Fig. 1.

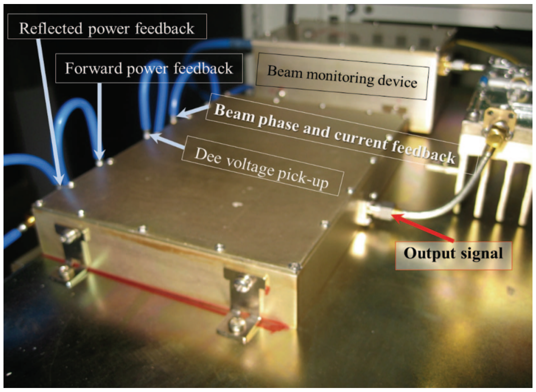

Fig. 1. (color online) The ILLRF with the feedback, output and beam-monitoring devices.

The RLC equivalent circuit of the cavity is taken into account, and if the frequency of the input signal is different from the resonant frequency of the cavity, then we will have reflected power that can be dangerous at maximum power. However, the RLC equivalent circuit of the cavity means that an input impedance is seen from the high power transmission line, consisting of a coupling capacitor, the cavity and a tuning capacitor.

2 Design of an intelligent low-level RF system

The reflected power causes a decrease in the signal amplitude in the Dees. Consequently, we should increase the assurance factor by measuring the signal amplitude of the Dees to analyze the resonant frequency of the cavity in addition to measuring the reflected power and the phase variations (the phase difference of the Dees' pick-up voltage and forward signal).

If there is an imbalance between the phase of the electric field in the interior of the cavity and the phase of the particle motion, we will not have an exterior beam.

As result, a beam-monitoring device is vitally important in order to use the ILLRF next to a pulsed ion source.

The microcontroller controls the ILLRF through feedback loops. For the initial configuration before startup, the designed working frequency of the cyclotron will be sent to the microcontroller through the serial interface.

2.1 Signal generation

The input clock frequency of the direct digital synthesizer (DDS) is established using a temperature-controlled crystal oscillator (TCXO), and the output frequency is a fraction of the input clock frequency [3]. The generation path, the adjustment of the RF signal, and the protection of the system can be observed in the block diagram in Fig. 2.

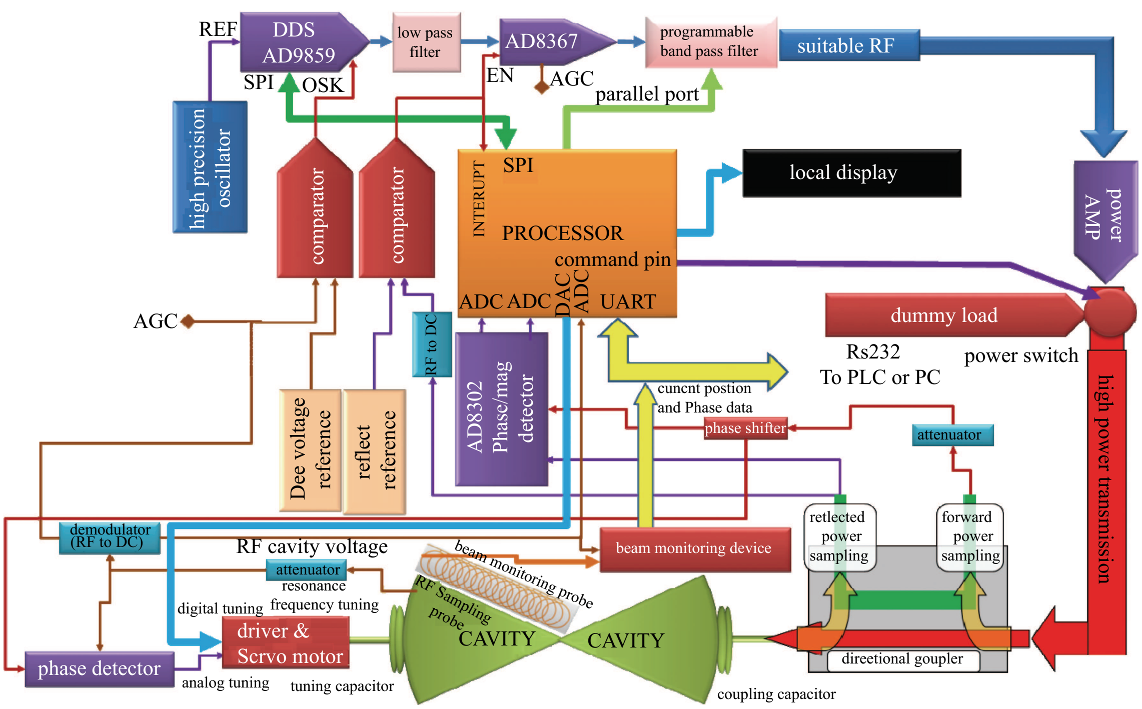

Fig. 2. (color online) ILLRF circuit block diagram and its connection to other parts of the RF set.

The microcontroller sends commands through a serial peripheral interface bus (SPI) to change the phase and the frequency of the DDS [4]. The analog signal in the DDS will be produced digitally. Therefore, the output consists of the fundamental signal and its harmonics. The ILLRF has two filters to eliminate noise and harmonics. First, a low-pass filter is placed after the DDS output [3], and a second narrow-band tunable band-pass filter is placed after the preamplifier to remove amplified residual noise and harmonics. The stability of the amplitude in the amplified signal of the Dees is related to the stability of the LLRF and the power amplifier amplitude, so according to the block diagram of Fig. 2, the Dees' pick-up signal amplitude is measured by the ADC and is recorded in the microprocessor. The local microprocessor then reports it to the main processor, as shown in the operation flowchart of Fig. 3. Simultaneously, the output level and amplitude stability are controlled by sending the output from the RF to the DC demodulator into the AGC of the preamplifier.

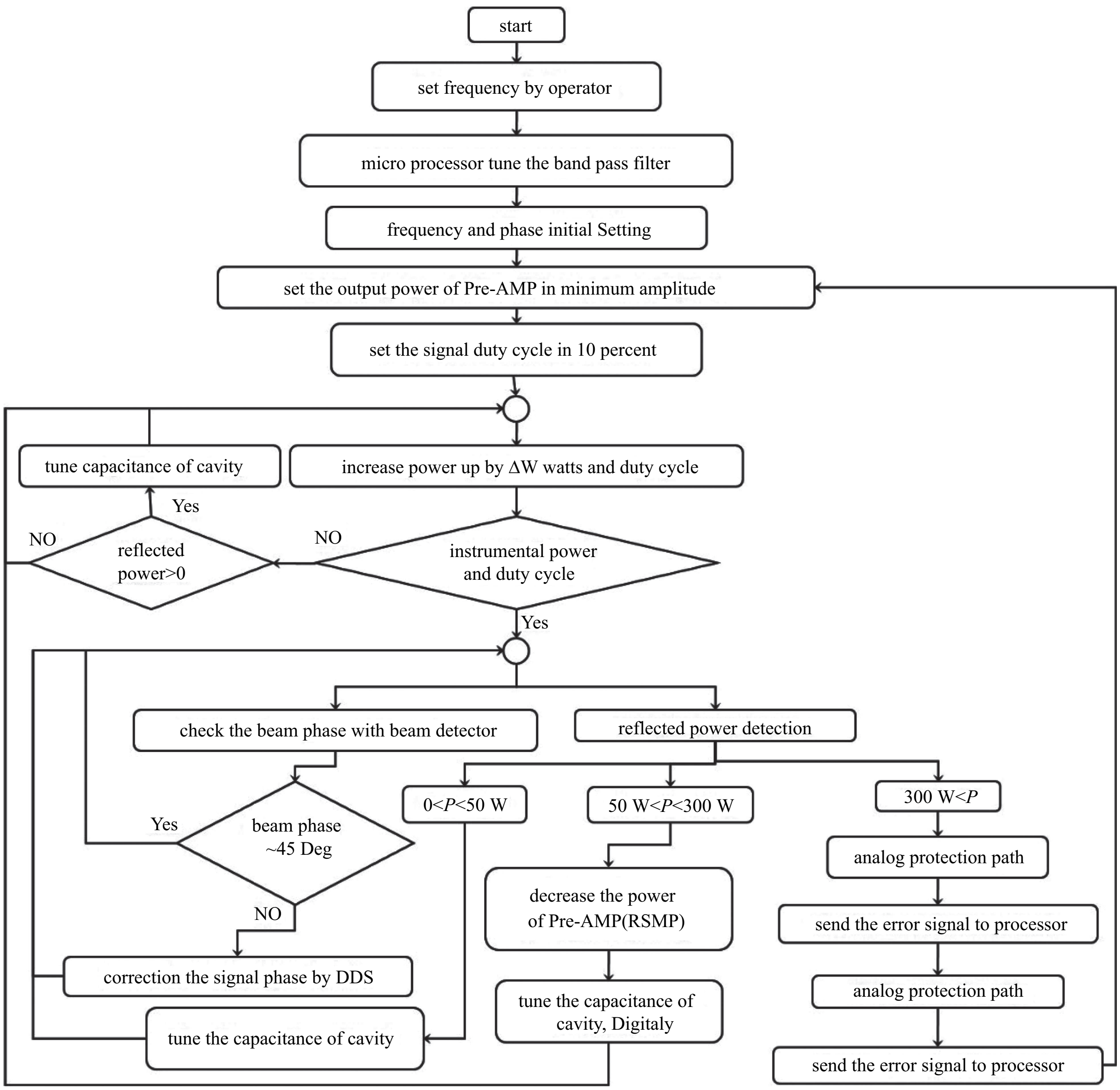

Fig. 3. ILLRF operation flowchart.

2.2 Startup process

The multipacting effect and mismatch, sparks and instability during the startup process must be addressed. To this end, the microcontroller will first set the output signal amplitude at the lowest level with a 10 percent duty cycle, and the phase difference of the Dees' pick-up voltage and amplified signal are then measured to adjust the tuning capacitor. Slowly and with the appropriate slope, the duty cycle is increased to 100 percent and the power to the maximum. Then, the Dees' signal amplitude, the reflected power and the phase difference are analyzed to readjust the resonant frequency.

2.3 Protection and readjustment process

After the startup has been completed, the tasks for the ILLRF include the non-stop analysis of the accuracy of the task, protection, correction of the initial settings, and the transmission of the beam and signal data to the main processor of the cyclotron. For protection, when the reflected power is more than 50 W and less than 300 W, the amplitude of the amplified signal is decreased to prevent the devastating effects of the reflected power and is then increased again after correcting the resonant frequency of the cavity. If the resonant frequency of the cavity is not corrected, then the critical level of the phase and amplitude of the reflected power are diagnosed. If the variation in the phase is more than 11.5 degrees or if the reflected power increases to more than 300 W, the signal is deflected to a dummy load by using a high power switch.

2.4 Amplitude stability

The amplitude stability of the amplified signal is related to the amplitude stability of the ILLRF and the power-amplifier, so the two errors decrease the sustainability of the system. Therefore, the ILLRF compensates for the error in the amplitude of the power-amplifier by implementing Dee amplitude feedback and AD8367 automatic gain control.

2.5 Variations and correction of resonance frequency

To detect the difference in the frequency between the resonant frequency of the cavity and the RF signal frequency, a sampling procedure is established for the forward and reflected power by using a directional-coupler. The Dees' signal is sampled by an antenna, and these signals in both the digital and analog paths are then analyzed. However, Pengzhan Li et al recently reported that the reflected power and the Dee amplitude signals are used only for protection [5]. The main path of the resonant frequency correction is the analogue path, and digital correction is for safety and stability. In the analogue path, the phase difference of the Dees' pick-up signal of the sampling antenna and the amplified signal of the directional-coupler are detected by the AD8302 phase detector [6], and the tuner capacitor is directly tuned by a servo motor. For the digital path, the Dees' amplitude and the reflected maximum range of the analogue correction is of 2°, so if the microcontroller detects a reflected power of more than 50 W, which is equivalent to 2° (according to the diagram in Fig. 4), the resonant frequency of the cavity will be digitally adjusted by tuning the capacitor. For the protection path, the amplitude of the reflected power is continuously compared to the level of the reference reflected power.

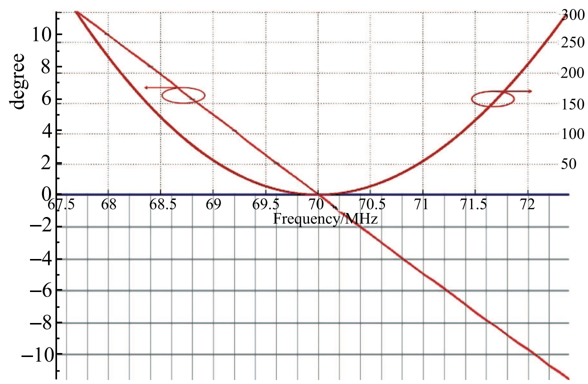

Fig. 4. (color online) The relationship between the phase difference and the reflected power for various frequencies which was simulated by MATLAB code.

Taking into account the RLC equivalent circuit of the cavity and the RF signal frequency, the reflected power levels in Eq. (1) are easily attainable.

$$\begin{aligned} P_{\text{ref}} &= P_{\text{fwd}} - P_{\text{loss}} \\ &= P_{\text{fwd}} - P_{\text{fwd}} \times \left| \frac{R}{R + \left(LW - \dfrac{1}{CW} \right) j} \right| . \end{aligned} \tag{1}$$

Only the magnitude of the variation of the resonant frequency of the cavity can be found with the use of the reflected power. However, according to the diagram in Fig. 4, the phase difference between the Dees' pick-up signal and forward power can be used to determine the variation in the resonant frequency by the magnitude and sign. The specifications of the AD8302 phase detector [6] indicate that the best response is at ±90°.

The reference phase is the phase difference of the forward power and the RF cavity signal at the resonant frequency. So the reference phase is transferred to 90° by using a phase shifter.

In addition to the reflected power and the phase difference, the third method to detect the variation in the resonant frequency is to analyze the signal amplitude inside of the Dees, which is the last option to protect the RF set.

2.6 Operation flowchart

The error signal is divided into 4 levels according to the variation rate of the resonant frequency, as shown in the diagram in Fig. 3.

First level: zero to 50 W of reflected power is equal to approximately 2° of phase difference, according to the diagram in Fig. 4. This is equal to a ±1 MHz difference from the working frequency. After detecting the variation in the resonant frequency, the analogue path tunes the resonant frequency of the cavity by tuning the capacitor. To eliminate errors in the first level, there is no need to change the transmitted power because the reflected power is very small and is not considered to be of any danger.

Second level: 50 to 300 W of reflected power. At first, the level of the signal amplitude decreases with the proper slope, and the resonant frequency of the cavity is then digitally adjusted. However, if the digital path is unable to detect the change in the resonant frequency or to make the necessary adjustments, then it minimizes the amplitude of the signal with a steep slope through the analog path to avoid probable danger.

Third level: More than 300 W of reflected power is equal to a phase difference of 11.5°. This level is 2 percent of the forward power and is equal to a ±2.25 MHz difference from the operating frequency for emergency protection of the power amplifier. Therefore, the level of the signal amplitude independently reaches the minimum with a steep slope, and the error signal is transmitted to the microcontroller to restart the system.

The amplitude inside the Dees has been used in both analog and digital paths. In the analog path, the Dee signal amplitude is compared with the reference Dee voltage for protection. In the digital path, the detection of the variation rate in the frequency, which is a factor of the signal amplitude, is digitalized by the microcontroller and will tune resonant frequency of the cavity using a tuning capacitor [7]. As shown in the flowchart in Fig. 3, two threshold levels are considered at 2° and 11.5° to detect the reflected power and the Dees' pick-up voltage.

3 Principles of the non-destructive beam-monitoring device

The task of this device is to simultaneously derive the time, position and the current information of the beam. The best time to accelerate a particle is the 45° phase of the RF signal. Therefore, the difference between the beam turning phase and the RF signal phase distinguishes the proper or improper operation of the cyclotron. As a consequence, if we do not have an output beam, the last beam current and the phase information are very important during the maintenance procedure. This structure has an advantage in that it can be easily installed in the cyclotron to produce isochronous fields. As a result, we need to detect the beam current for the initial setup and also need to have complete control over the operation of the system. With the help of a Faraday cup, the beam current detection causes a blockage in the exit beam, but this detector detects the beam without causing any blockage by locating the beam probe in the valleys during the entire operation of accelerator, as shown in Fig. 5 [8].

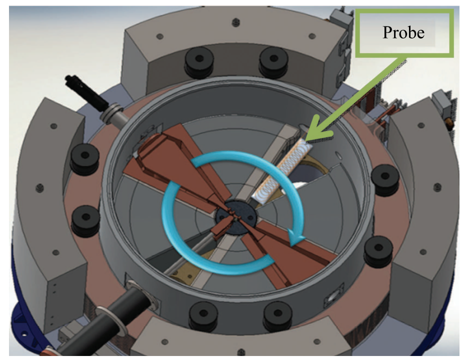

Fig. 5. (color online) Beam monitoring probe location in the space valleys.

A charged particle generates a magnetic field while it moves (as shown in Fig. 6). According to Eq. (2), the magnitude of this field is relative to the charge of the particle, the distance from the path, and the magnetic permittivity of the coefficient [9].

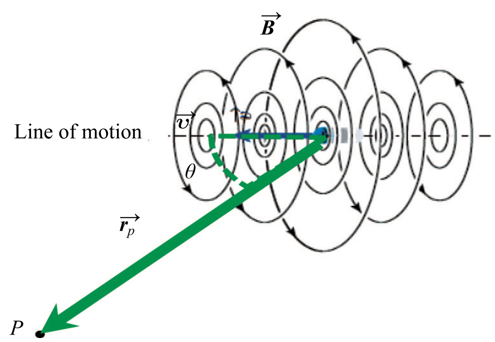

Fig. 6. (color online) Magnetic field caused by the motion of charged particles.

$$\vec{B} = \frac{\mu_0}{4\pi} \frac{q\vec{v} \times r_{\hat{P}_P}}{r^2_{P_P}}, \quad (2)$$

where r is the distance in meters, v is the speed in meters per second, and q is the charge in coulombs. The number of particles in each bunch in a cyclotron accelerator is about 1×10^6–1×10^8 particles. For example, we assume 5 MeV protons. To calculate the magnetic field, according to Eq. (3), the speed of each particle should first be calculated with

$$
\begin{aligned}
KE &= \frac{1}{2}\frac{m}{\sqrt{1-\left(\frac{v^2}{c^2}\right)}}V^2 = \frac{E}{6.241509\times10^{18}}\text{Joule},\\
V &= \frac{\left(1.41\times\sqrt{(KE\times\sqrt{(KE^2+c^4\times m^2)}-KE^2)}\right)}{c\times m}\\
&= 3.0864\times10^7\ \mathrm{m/s},
\end{aligned}
\tag{3}
$$

where m is the mass of the particle in grams (m=1.673×10^{-27}g), c is the speed of light, E is the energy of the particle, m is the relativistic mass of the particle, and KE is the kinetic energy. According to Eq. (3), the speed of a 5 MeV proton will be equal to 3.0864×10^7m/s, and we obtain the magnetic field from Eq. (2).

The equation $I = -N\Delta\varphi/\Delta t$ is used to assess the amount of current induced in the beam monitoring probe, and the magnetic flux at each spot will be calculated using Eq. (4). $\Delta\Phi$ will then be obtained by determining the flux at two spots. When the speed of the particle is clarified, the necessary time to move the particle from the first point to the second will become equal to Δt, and consequently, the maximum amplitude of the induced current will become equal to 28 μA by using a coil with an area of 4 cm^2.

In

$$\varphi = B\cdot A\cos(\theta) \tag{4}$$

where B is the magnetic field and A is the area of the coil. Contrary to the simulation, a spot beam is considered in the calculations to simplify the beam bunch. Therefore, the amplitude of the current that is induced becomes a little higher. The simulation was carried out in CST Particle Studio [10], and the current induced in the coils of the beam monitoring probe was studied with different cross-sections and equal areas, as shown in Fig. 7. In the literature, only one study has previously been presented on nondestructive phase detection [7]. Unfortunately, this work is not accurate even though it is a good contribution. According to the graphs shown in Fig. 8, which were obtained using CST Particle Studio, the optimal cross section from the coils is a circular cross section because its output signal has the highest induced current and the fastest zero crossing, contrary to the phase probe cross section reported by Satoru Hojo et al [8].

The graphs in Fig. 9 show the current induced in the single-looped coils with different distances relative to the path of the particle with a maximum induced current of about 18 μA. As the coils move some distance from the beam path, the induced current decreases. Consequently, these conditions can be used to detect the motional radius of the beam. The zero crossing time will be utilized as the reference for timing. To detect the magnitude of beam current at any moment, the magnitude of the current induced in the coils will be added up after being corrected. This calibration can thus be used to attribute the total current that is induced to the amount of the beam current.

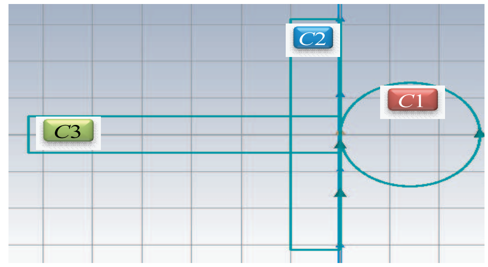

Fig. 7. (color online) Coils with different cross sections.

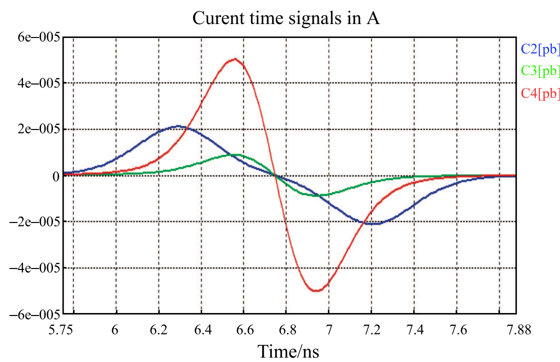

Fig. 8. (color online) Current induced in the coils of the beam monitoring probe with different cross-sectional areas.

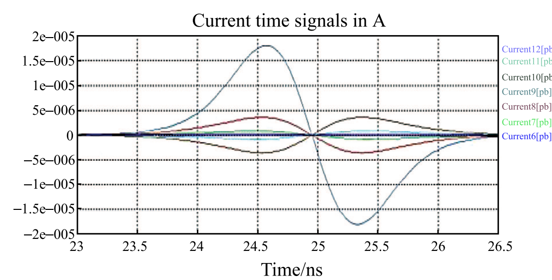

Fig. 9. (color online) Current induced in the single-loop coil with different distances.

4 Main sub-blocks of ILLRF

4.1 Variations and correction of resonance frequency

As a result of the use of appropriate sub-blocks, the level of processing in the microcontroller decreases, so there is no need to employ very high-speed microcontrollers. A microcontroller from the Atmel AVR ATmega family is sufficient, taking into account the necessary measures to reduce noise. On the other hand the

Digital signal processor or DSP was over-designed in recent work by Pengzhan Li et al [5]. To send the necessary data and to provide non-automated control by the operator, the microcontroller is connected to the main processor through a serial interface.

4.2 Direct digital synthesizer

The DDS with the TCXO crystal oscillator is responsible to generate the signal and adjust the signal phase and frequency. In this design, an AD9859 synthesizer is used instead of Voltage-controlled oscillator (VCO) and I-Q modulators, so the phase and frequency can be easily adjusted by the microcontroller [4].

4.3 The VGA preamplifier

To achieve a stable signal amplitude and to provide RF set protection, a preamplifier with automatic gain control and an AD8367 variable gain amplifier are utilized [11].

4.4 Filters

The DDS generates the analog signal by using digital techniques. Therefore, the harmonics of the generated signal will also appear. A suitable low-pass filter is used to ensure that the DDS output signal is quite clean and non-harmonic [2]. To decrease the noise and left-over harmonics and to provide more control and protection, a tunable ultra-narrow-band band-pass filter is used after the preamplifier.

4.5 Demodulator

To compare the power and the amplitude of the signal to the reference power and amplitude, an adequate signal amplitude is employed. Therefore the level of the sampled signal is first converted to a usable one with a fixed factor in order to reduce unwanted errors, and then the RF signal is converted to a DC voltage level by using the AD8361 [12] and AD736 [13] chips.

4.6 Beam-monitoring device description

A beam monitoring probe consisting of 88 coils is

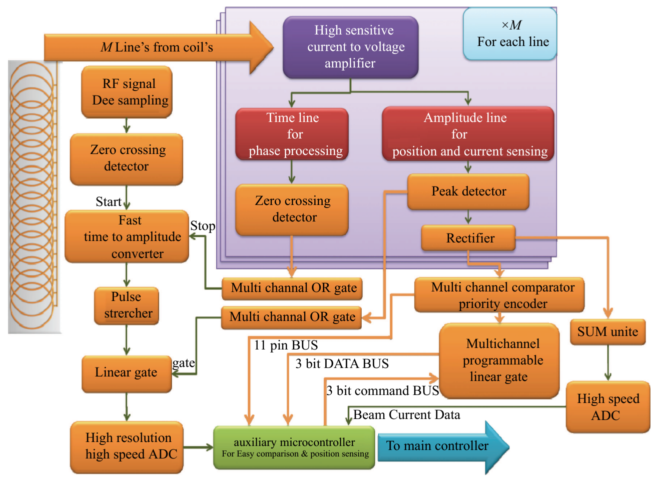

Fig. 10. (color online) Block diagram of the beam-monitoring device.

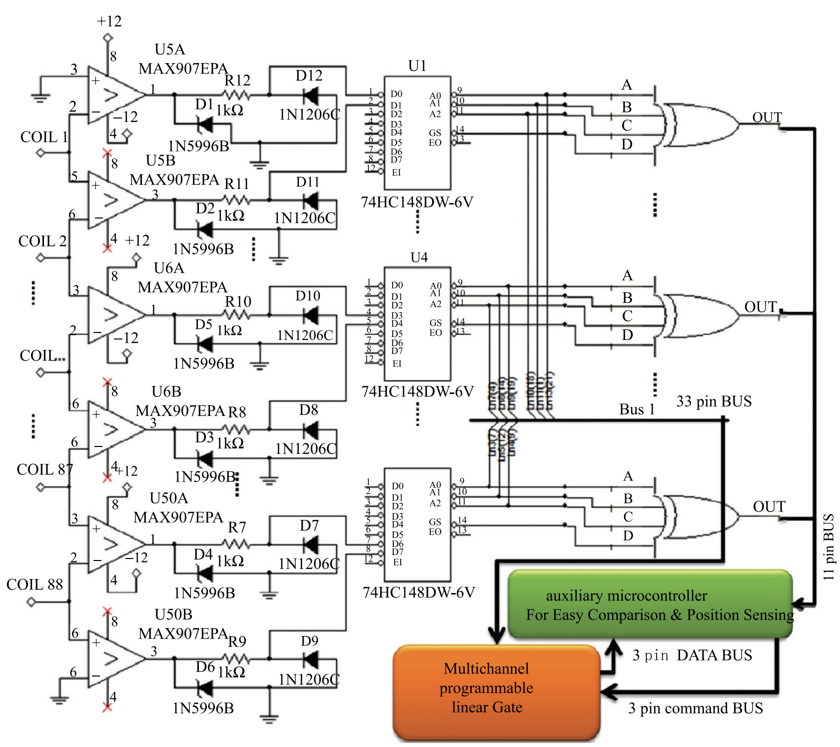

Fig. 11. (color online) 88 wire Parallel BUS converter to a 17 wire BUS with the use of a multichannel priority encoder comparator and multichannel programmable linear gate.

used to detect the turning radius. Therefore, M is equal to 88 in Fig. 10. The current induced in each coil in a high sensitive current to voltage amplifier converts the current to a voltage signal with the appropriate amplitude [14]. Then the signal is guided into two paths to acquire time-phase data and current-position data. To calculate the beam characteristics, an auxiliary processor is used to decrease the processing level of the main ILLRF microcontroller. On the obtained time data path, the zero crossing time is the timing reference. Consequently, the zero crossing time of the Biopsied RF signal is used to startup the Time-to-Amplitude Converter or the TAC. Then, the zero crossing time of the induced current will stop the TAC.

To reduce the noise effects, timing is synchronized between the zero crossing detector of the induced current and the induced current of the peak detector. The output amplitude of the TAC is converted to digital data and is then sent to the auxiliary microcontroller.

To acquire the current data, the rectified amplitude of the coils is collected by the SUM unit after digitalization is sent to the auxiliary microcontroller. On the path to extract the position-radius data, the coil with the highest amplitude of the induced current represents the motion radius of the beam. Therefore, the maximum amplitude is detected by the comparator, and the number of coils with the maximum amplitude is sent to the auxiliary microcontroller as an indicator of the motion radius. For this purpose, an 88 wire Parallel BUS is required, and a 100-pin microcontroller is also needed.

However, as seen in Fig. 11, the Multichannel Priority Encoder Comparator and Multichannel Programmable Linear Gate are used to reduce the connecting path of the coils to the auxiliary microcontroller to a 17 wire BUS by using the SN74HC148 8-Line To 3-Line Priority Encoders [15].

5 Conclusion

A circuit was designed to minimize the level of noise and harmonics by using a tunable narrow band-pass filter for a wide range of RF accelerators. This system has no limitation in terms of reducing the bandwidth of the output, as in telecommunication systems based on synthesizers. It is vital to protect the bandwidth when an ILLRF is used for a wide range of RF accelerators, and this characteristic has been entirely realized in this work.

Table 1. RF test results and some characteristics of this cyclotron.

parameter	value
operating RF frequency	70 MHz
RF output power	15 kW
magnetic field between upper and lower magnet pole	0.26 up to 1.83 T
RF frequency tolerance @−40 to +85℃	±1.75 kHz
RF frequency tolerance @+25℃	±350 Hz
Dee voltage stability	$\pm 7\times 10^{-4}$
max VSWR	<1.3179
phase error	$<\pm 0.63°$
minimum detectable resonance frequency variation	< 200 kHz
operating temperature	−40℃ to +85℃
typical temperature	25℃
second-order harmonic distortion	−58 dBc

The open loop RF generation and the adjustment have been tested, and the results of RF tests and some of the characteristics of this cyclotron have been demonstrated in Table 1.

References

1 K Liu et al, *Proc. of IPAC*, particle accelerator, San Sebastian, Spain, (2011) 1753
2 S Turner, CAS –CERN Accelerator School, (1992) 437
3 Analog Devices: AD9859 Datasheet, Analog Devices, Inc. (2009) 24
4 A Caruso et al, *Proc. of CYCLOTRONS*, Lanzhou, China, (2010) 159
5 P Li et al, Nucl. Instrum. Methods A, **735**: 184 (2014)
6 Analog Devices: AD8302 Datasheet, Analog Devices, Inc. (2002) 24
7 X Wang et al, Nucl. Instrum. Meth B, (2007) 26
8 S Hojo et al, in: IBIC 2012, Tsukuba, Japan, (2012) 60
9 E Mazur, *The Principles and Practice of Physics*, CHAPTER 28, (2014)
10 CST PARTICLE STUDIO$^{\mathrm{TM}}$, 2014, http://www.cst.com
11 Analog Devices: AD8367 Datasheet, Analog Devices, Inc. (2001) 16.
12 Analog Devices: AD8361 Datasheet, Analog Devices, Inc. (2004) 16.
13 Analog Devices: AD736 Datasheet. Analog Devices, Inc. (2012) 20.
14 Wang C, *3rd International Design and Test Workshop*, IDT **354**: 357 (2008)
15 Texas Instruments: SN74HC148 Datasheet, (2004)